Journal of Alloys and Compounds 506 (2010) 88–92

Contents lists available at ScienceDirect

Journal of Alloys and Compounds

journal homepage: www.elsevier.com/locate/jallcom

Microstructure and thermal stability of amorphous SiBCNAl powders fabricated by mechanical alloying

Dan Ye, De-Chang Jia *, Zhi-Hua Yang, Zhen-Lin Sun, Peng-Fei Zhang

Institute for Advanced Ceramics, Department of Materials Science, Harbin Institute of Technology, No. 92, West Da-Zhi Street, Harbin 150001, China

ARTICLE INFO

Article history:
Received 8 February 2010
Received in revised form 25 June 2010
Accepted 30 June 2010
Available online 8 July 2010

Keywords:
Amorphous materials
Mechanical alloying
Microstructure
Thermal analysis

ABSTRACT

Amorphous SiBCNAl powders have been prepared by mechanical alloying (MA) technique using crystalline silicon (Si), hexagonal boron nitride (h-BN), graphite (C) and aluminum (Al) as starting materials. Microstructural characterization was carried out by X-ray diffraction (XRD), transmission electron microscopy (TEM), high-resolution transmission electron microscopy (HRTEM) and selected area diffraction (SAD). The results showed that the MA SiBCNAl powders were completely amorphous and no nanocrystalline structure had been detected. ^{29}Si and ^{27}Al solid-state nuclear magnetic resonance (NMR) spectra have provided evidence that Si and C atoms are intimately mixed at atomic levels and aluminium is present as mixed AlN_4, AlN_5/AlO_4 and AlN_6 units. Structural characterization by X-ray photoelectron spectroscopy (XPS) has shown the coexistence of chemical bonds formed by reactions of element of Si, B, C, N and Al. The thermal stability of SiBCNAl powders has been analyzed by thermogravimetry in argon.

1. Introduction

SiBCN precursor-derived ceramics are promising candidates for high-temperature structural applications because of their outstanding high-temperature stability [1], high oxidation resistance [2] and mechanical properties [3–5]. However, oxidation times exceeding 24 h at 1500 °C led to crystallization of the formerly amorphous oxide scales with concurrent bubble formation [6] because of volatilisation of boron species. Similar observations were reported from the high-temperature oxidation of sintered SiC containing boron as a sintering additive [7]. To improve the scale quality, Müller et al. prepared a new kind of SiBCNAl precursor-derived ceramics and investigated their oxidation behaviour [8]. It was found that the addition of aluminium had a beneficial effect indeed on impeding bubble formation as well as cracking and spallation of the oxide scales.

Nowadays, the synthesis and pyrolysis of precursors need to be done in inert gases, and the corresponding processes are very complicated and the starting materials are very expensive, so it is necessary to find other routes of synthesis for SiBCNAl powders and ceramics. Powder processing by mechanical alloying (MA) has attracted wide practical interest as it offers a simple but powerful way to synthesize non-equilibrium phases and microstructures, from nanograin materials to extended solid solutions, amorphous phases, chemically disordered compounds and nanocomposites [9]. Solid-state amorphization (SSA, or crystalline-to-amorphous phase transformation) by mechanical alloying involves deformation at much high strain rate, cold welding, fragmentation and dynamic recrystallization [10]. For the microstructure produced by mechanical attrition, the strain and lattice disorder can be retained in highly metastable state [11]. As a result, the composition range for amorphization is usually much greater by mechanically driven processes than that by other techniques, such as rapid solidification.

SiC [12–14], BCN [15–17], AlN [18,19] and SiBCN [20] powders have been fabricated by MA. However, work on the synthesis of SiBCNAl powders by solid-state reaction has not been reported yet. Thus, a new way of fabricating amorphous SiBCNAl powders has been suggested in this paper for the first time.

2. Experimental

Commercially available crystalline silicon (c-Si, ca. 15 μm, >99.5% pure), hexagonal boron nitride (h-BN, ca. 0.6 μm, >98% pure), graphite (C, ca. 4 μm, >99.9% pure) and aluminum (Al, ca. 3 μm, 99.9% pure) powders were used as starting materials for high-energy ball milling. The powders were mixed at the ratio of Si:BN:C:Al = 1:0.5:1.5:0.3 to give a composition of $SiB_{0.5}C_{1.5}N_{0.5}Al_{0.3}$ and then mechanically alloyed in a high-energy planetary ball mill (Fritsch Pulverisette 4, Germany) using silicon nitride (Si_3N_4) vials and silicon nitride balls (10 mm in diameter). The MA was carried out with a ball-to-powder mass ratio (B/P) of 30:1 for 5, 15 and 25 h, respectively. After each hour, the milling was stopped for 30 min. In the following experiments, without special notification, mechanical alloying was done for 25 h. All transfers of powders to and from the vials were done in a glove box filled with pure (99.99%) argon. The vial was then sealed and transferred to a planetary ball mill.

The structural characterization of powders was analyzed using X-ray diffraction (XRD) methods with Cu Kα radiation. Particle morphology observation was performed on a Tecnai F30 field emission gun transmission electron microscope (TEM). The results of the XRD analysis concerning amorphization were verified by

---

* Corresponding author. Tel.: +86 451 86418792; fax: +86 451 86414291.
E-mail address: dchjia@yahoo.com.cn (D.-C. Jia).

0925-8388/$ – see front matter © 2010 Elsevier B.V. All rights reserved.
doi:10.1016/j.jallcom.2010.06.176

high-resolution transmission electron microscopy (HRTEM) using a Tecnai F30 TEM instrument operated at 300 kV and selected area diffraction (SAD). The X-ray photoelectron spectroscopy (XPS) analysis was performed on a PHI ESCA system using Al Kα radiation ($h\nu$ = 1486.6 eV). The signal curves were fitted by deconvolutions of peaks using Gaussian–Lorenzian peak approximations and Shirley background reduction. ^{29}Si and ^{27}Al solid-state magic angle spinning (MAS) nuclear magnetic resonance (NMR) spectra were recorded on a Bruker Avance III 400 spectrometer, operating at 79.3 MHz for Si and 104 MHz for Al. The magic angle was set using the ^{79}Br resonance of KBr. Zirconia pencil rotors were used, and spun at the magic angle with a spinning rate of 5 kHz for Si and 12 kHz for Al. ^{27}Al spectra were referenced to aqueous $Al(NO_3)_3$ (0 ppm). ^{29}Si spectra were referenced to tetrakis-trimethylsilyl-silane, which was itself referenced to tetramethylsilane (TMS) at 0 ppm. Thermogravimetric analysis (TGA) of the powders was performed in an Al_2O_3 crucible (STA-449C, Netzsch) from room temperature to 1500 °C at heating rates of 10 °C/min in argon.

3. Results and discussion

In an attempt to prepare amorphous SiBCNAl powders, a set of experiments with different milling times were conducted. Fig. 1 shows the XRD patterns of SiBCNAl powders milled for different milling times (0, 5, 15 and 25 h). As it is shown, the diffraction peaks of BN, C and Al disappear completely while those of crystalline Si still exist beyond 5 h of milling. This indicates that amorphization of BN, C and Al is easier than that of Si. After 15 h of milling, the diffraction peaks of Si obviously decrease in intensity. When the milling time is up to 25 h, a halo peak corresponding to an amorphous phase is observed and the sample can be considered as completely X-ray amorphous.

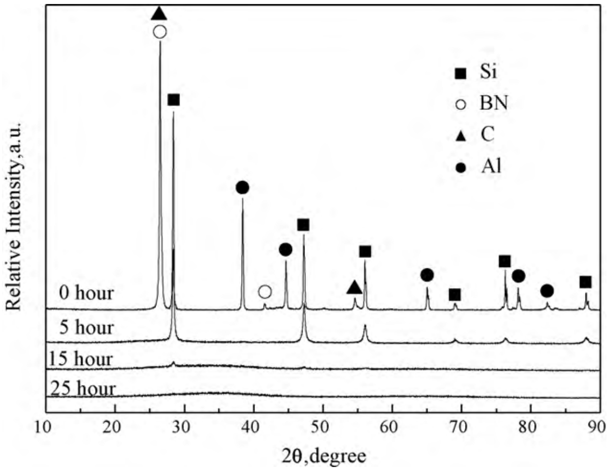

Fig. 1. XRD patterns of SiBCNAl powders milled for different times.

The TEM image of SiBCNAl powders is shown in Fig. 2(a). It can be seen that the size of particles is of the order of 100–200 nm. It should be noted that the small particles and the edge of the large particles of the bright-field images are featureless, suggesting that these small particles and the edge of large particles might be amorphous. Such conjecture is consistent with the SAD pattern (Fig. 2(b)) that exhibits a broad and diffused halo suggesting the presence of amorphous phases.

A mass of observations on SiBCNAl powder particles by using high-resolution transmission electron microscope show that the particles are completely amorphous and no nanocrystalline struc-

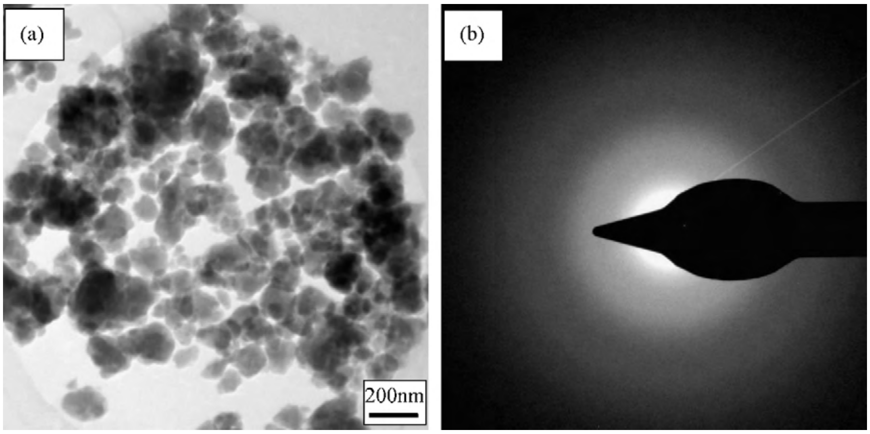

Fig. 2. (a) TEM image and (b) the corresponding SAD pattern of SiBCNAl powders.

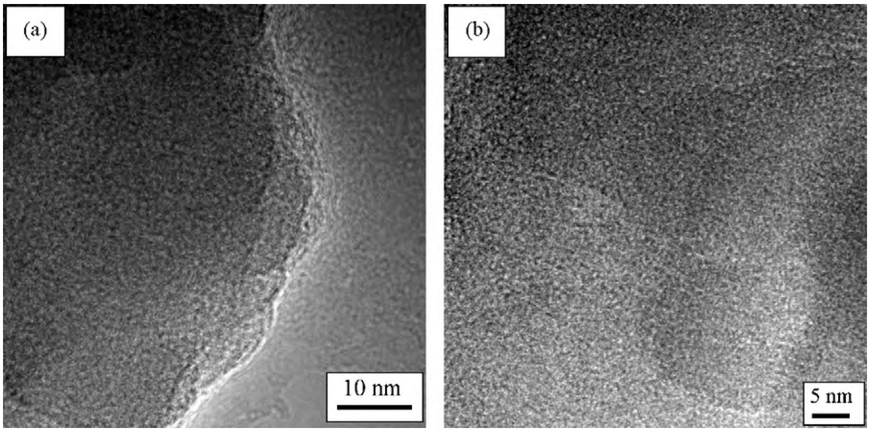

Fig. 3. Typical HRTEM images of SiBCNAl powder particles: (a) the edge of a particle and (b) the center area of a particle.

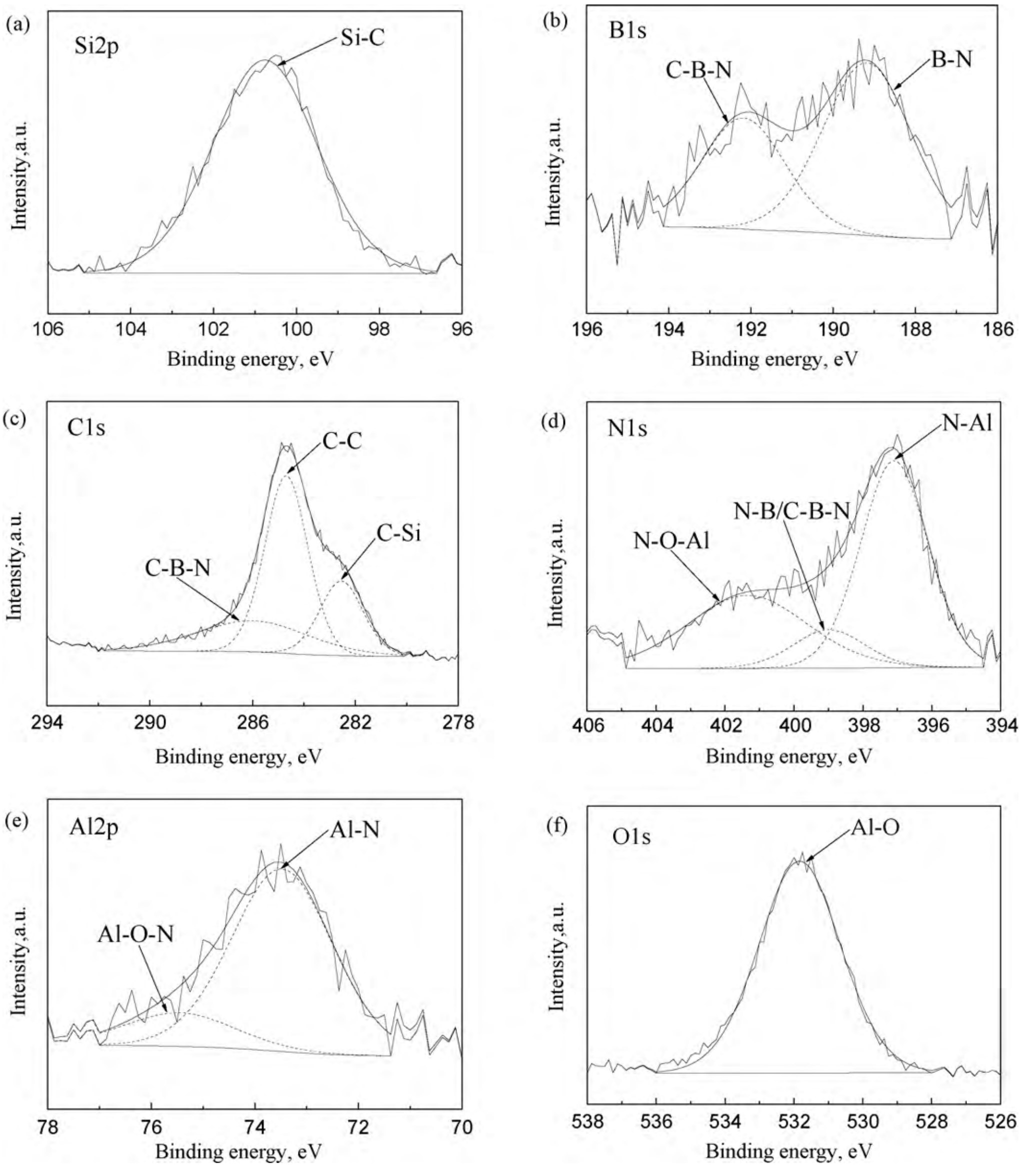

Fig. 4. (a) Si2p, (b) B1s, (c) C1s, (d) N1s, (e) Al2p and (f) O1s XPS spectra, with deconvolutions of peaks, recorded for SiBCNAl powders.

ture has been detected anywhere in the specimen, thus supporting the XRD and TEM results. Fig. 3 gives typical HRTEM images of SiBCNAl powder particles.

In order to further investigate the SiBCNAl powders at atomic level, the XPS and NMR studies were conducted. XPS analysis can give direct information about the bonding type of the atoms in solid phases. The XPS measurement results of the as-prepared SiBCNAl powders are shown in Fig. 4. The characteristic peaks at 100.8 eV (Si2p) and 282.5 eV (C1s) were assigned to the Si–C bonds of SiC [21]. The peaks at 192.2 eV (B1s), 286.1 eV (C1s) and 398.9 eV (N1s) can reflect the existence of B–C–N bonds [22]. There is a peak at 284.6 eV for C1s spectrum, which was assigned to the C–C bonds of graphite and agreed well with result of starting graphite [21]. The peaks at 189.3 eV (B1s) and 398.9 eV (N1s) may be assigned to the B–N bonds of h-BN [22]. The characteristic peaks at 73.5 eV and 397 eV were identified as Al2p and N1s signals of the Al–N bond, respectively [23,24]. The peaks at 75.6 eV (Al2p), 531.7 eV (O1s) and 401.6 eV (N1s) may reflect the existence of Al–O–N bonds [25–27]. The O element in Al–O–N bond may be derived from Al_2O_3 covering the surfaces of the Al particles used as starting material and a trace amount of oxygen in the argon gas used in the milling. The amount of oxygen is 2.62 wt.% (as shown in Table 1). Structural characterization by XPS revealed the coexistence of chemical bonds formed by reactions of element of Si, B, C, N and Al. The as-fabricated SiBCNAl powders appeared to possess a structure containing hybridization of several bonds such as Si–C, B–C–N, C–C, B–N and Al–N, rather than a simple complex of these bonds.

Table 1
Compositional characteristics of the MA SiBCNAl powders.

Elemental analysis (mass%)							Compositional formula
Si	B	C	N	Al	O	Total	
40.46	7.80	26.82	10.48	11.51	2.62	99.69	$SiB_{0.49}C_{1.54}N_{0.51}Al_{0.29}O_{0.11}$

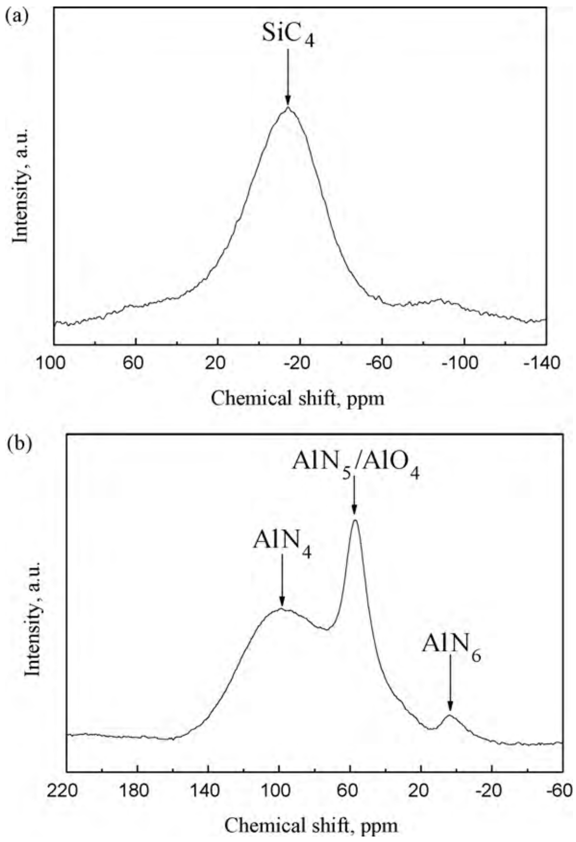

Fig. 5. (a) ^{29}Si and (b) ^{27}Al NMR spectra of the SiBCNAl powders.

Solid-state NMR spectroscopy can be used to probe the local environment (short-range order up to a few Å) around selected nuclei and is applicable for the characterization of even amorphous systems [28]. ^{29}Si and ^{27}Al solid-state NMR spectra of the SiBCNAl powders are shown in Fig. 5. ^{29}Si NMR spectrum (as indicated in Fig. 5(a)) shows a broad peak around −15 ppm characteristic of an amorphous SiC structure based on SiC_4 sites and a small hump at −85 ppm suggesting the presence of a small amount of amorphous Si due to insufficient milling [13]. The result indicates that Si and C atoms are intimately mixed at atomic levels in the amorphous phase. Three signals centered at 100, 57 and 4 ppm are observed in the ^{27}Al NMR spectrum (Fig. 5(b)). The 100 ppm signal corresponds to tetrahedral AlN_4 sites [29], implying the presence of AlN in the as-milled powders. The position of the resonance at 57 ppm may be assigned to the mixed local chemical environment of the aluminium nuclei corresponding to pentahedral AlN_5 and/or tetrahedral AlO_4 units [30,31]. A small peak at 4 ppm should be responded to octahedral AlN_6 units [31]. From the data deduced from the ^{27}Al solid-state NMR spectra, we can conclude that aluminium is present as mixed AlN_4, AlN_5/AlO_4 and AlN_6 units.

Fig. 6 shows the thermal stability of the SiBCNAl powders which was analyzed by TGA in argon. The powders exhibit excellent thermal stability in argon with a very small mass loss of 2.13% at 1500 °C. The mass loss of the powders occurred only after ∼1350 °C and should be attributed to the reduction reaction of SiO_2 and Al_2O_3 covering the surfaces of the Si and Al particles used as starting materials. The possible reduction reactions are represented by reactions (1)–(6) [32,33]:

$$SiO_2(s) + 2SiC(s) \rightarrow 3Si(s) + 2CO(g) \quad (1)$$

$$2SiO_2(s) + SiC(s) \rightarrow 3SiO(g) + CO(g) \quad (2)$$

$$SiO_2(s) + C(s) \rightarrow SiC(s) + CO(g) \quad \text{and/or} \quad CO_2(g) \quad (3)$$

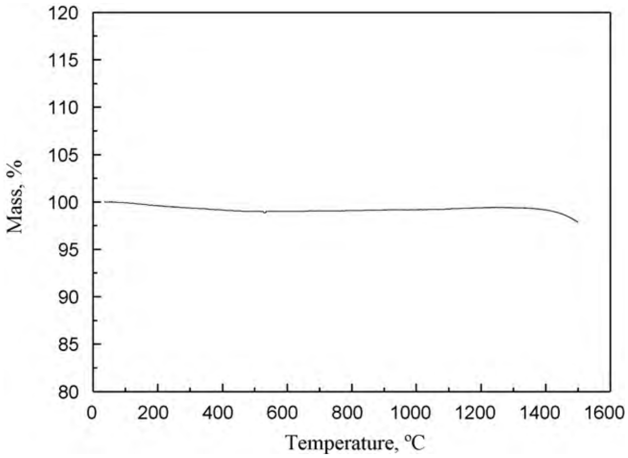

Fig. 6. TGA curves for the SiBCNAl powders in argon.

$$SiO_2(s) + C(s) \rightarrow SiO(g) + CO(g) \quad \text{and/or} \quad CO_2(g) \quad (4)$$

$$Al_2O_3(s) + C(s) \rightarrow Al_2O(g) + CO(g) \quad \text{and/or} \quad CO_2(g) \quad (5)$$

$$Al_2O_3(s) + C(s) \rightarrow Al_2OC(s) + CO(g) \quad \text{and/or} \quad CO_2(g) \quad (6)$$

4. Conclusions

From the present study, it appears that amorphous SiBCNAl powders have been fabricated by high-energy ball milling using crystalline Si, h-BN, C and Al and elements of Si, B, C, N and Al compounded at atom level. The synthesized SiBCNAl powders appeared to possess a structure containing hybridization of several bonds such as Si–C, B–C–N, C–C, B–N and Al–N, rather than a simple complex of these bonds. The thermal stability of SiBCNAl powders was excellent at high temperature in argon.

Acknowledgments

This work was financially supported by the National Natural Science Foundation of China (NSFC, Grant number 50902031) and Project Supported by Development Program for Outstanding Young Teachers in Harbin Institute of Technology (HITQNJS.2009.064).

References

[1] R. Riedel, A. Kienzle, W. Dressler, L. Ruwisch, J. Bill, F. Aldinger, Nature 382 (1996) 796–798.
[2] H.P. Baldus, M. Jansen, Angew. Chem. Int. Ed. Engl. 36 (1997) 328–343.
[3] R. Riedel, L.M. Ruswisch, L. An, R. Raj, J. Am. Ceram. Soc. 81 (1998) 3341–3344.
[4] M. Christ, G. Thurn, M. Weinmann, J. Bill, F. Aldinger, J. Am. Ceram. Soc. 83 (2000) 3025–3032.
[5] M. Jansen, B. Jäschke, T. Jäschke, Structure & Bonding: High Performance Non-oxide Ceramics I, Springer Berlin, Inc., Heidelberg, 2002, pp. 137–191.
[6] E. Butchereit, K.G. Nickel, A. Müller, J. Am. Ceram. Soc. 84 (2001) 2184–2188.
[7] C. Schumacher, PhD thesis, Universität Tübingen (2001).
[8] A. Müller, P. Gerstel, E. Butchereit, K.G. Nickel, F. Aldinger, J. Eur. Ceram. Soc. 24 (2004) 3409–3417.
[9] C. Suryanarayana, Prog. Mater. Sci. 46 (2001) 1–184.
[10] H.J. Fecht, in: C.C. Koch (Ed.), Nanostructured Materials: Processing, Properties, and Applications, Noyes Publication, William Andrew Publishing, Inc., New York, 2002, p. 73.
[11] D.L. Zhang, Prog. Mater. Sci. 49 (2004) 537–560.
[12] X.Y. Yang, Z.W. Huang, Y.K. Wu, H.Q. Ye, Mater. Sci. Eng. A 300 (2001) 278–283.
[13] X.Q. Xie, Z.G. Yang, R. Ren, L.L. Shaw, Mater. Sci. Eng. A 255 (1998) 39–48.
[14] B. Ghosh, S.K. Pradhan, J. Alloys Compd. 486 (2009) 480–485.
[15] R. Torres, I. Caretti, R. Gago, Z. Martín, I. Jiménez, Diamond Relat. Mater. 16 (2007) 1450–1454.
[16] B. Yao, L. Liu, W.H. Su, J. Appl. Phys. 86 (1999) 2464–2467.
[17] Y.F. Zhang, Y.H. Tang, C.S. Lee, I. Bello, S.T. Lee, Diamond Relat. Mater. 8 (1999) 610–613.
[18] Y.J. Du, S.Y. Li, K. Zhang, K. Lu, Scripta Mater. 36 (1997) 7–14.
[19] Z.P. Xia, Z.Q. Li, C.J. Lu, B. Zhang, Y. Zhou, J. Alloys Compd. 399 (2005) 139–143.
[20] Z.H. Yang, D.C. Jia, Y. Zhou, C.Q. Yu, Ceram. Int. 33 (2007) 1573–1577.

[21] W.F.A. Besling, A. Goossens, B. Meester, J. Schoonman, J. Appl. Phys. 83 (1998) 544–553.
[22] Y.H. Xiong, C.S. Xiong, S.Q. Wei, H.W. Yang, Y.T. Mai, W. Xu, S. Yang, G.H. Dai, S.J. Song, J. Xiong, Z.M. Ren, J. Zhang, H.L. Pi, Z.C. Xia, S.L. Yuan, Appl. Surf. Sci. 253 (2006) 2515–2521.
[23] F. Malengreau, V. Hautier, M. Vermeersch, R. Sporken, R. Caudano, Surf. Sci. 330 (1995) 75–85.
[24] R. Dalmau, R. Collazo, S. Mita, Z. Sitar, J. Electron. Mater. 36 (2007) 414–419.
[25] T. Do, N.S. McIntyre, R.A. Harshman, M.E. Lundy, S.J. Splinter, Surf. Interf. Anal. 27 (1999) 618–628.
[26] J.F. Moulder, Handbook of X-ray Photoelectron Spectroscopy, Perkin-Elmer, Minnesota, 1992.
[27] G.V. Soares, K.P. Bastos, R.P. Pezzi, L. Miotti, C. Driemeier, I.J.R. Baumvol, C. Hinkle, G. Lucovsky, Appl. Phys. Lett. 84 (2004) 4992–4994.
[28] K. Schmidt-Rohr, H.W. Spiess, Multidimensional Solid-state NMR and Polymers, Academic Press, London, 1994.
[29] F. Berger, M. Weinmann, F. Aldinger, K. Müller, Chem. Mater. 16 (2004) 919–929.
[30] R. Toyoda, S. Kitaoka, Y. Sugahara, J. Eur. Ceram. Soc. 28 (2008) 271–277.
[31] X.D. Li, M.J. Edirisinghe, J. Am. Ceram. Soc. 86 (2003) 2212–2214.
[32] W.J. Clegg, J. Am. Ceram. Soc. 83 (2000) 1039–1043.
[33] G.-J. Zhang, J.-F. Yang, T. Ohji, J. Am. Ceram. Soc. 85 (2002) 2256–2260.